Heat-flux scaling for weakly forced turbulent convection in the atmosphere

By KUSUMA G. RAO[1] AND R. NARASIMHA[2]

[1]Space Sciences, Indian Space Research Organization, Bangalore 560 094, India

[2]Jawaharlal Nehru Centre for Advanced Scientific Research, Bangalore 560 064, India
roddam@caos.iisc.ernet.in

Observational data in the atmosphere indicate that conventionally defined drag and heat transfer coefficients increase rapidly as wind speed falls. It is shown here that, at sufficiently low wind speeds, the observed heat flux is nearly independent of wind speed but the drag increases linearly with it. These findings are not consistent with the free-convection limit of the Businger relations for Monin–Obukhov theory, and lend support to the ideas of Ingersoll (1966) and Grachev (1990), till now checked only against laboratory experiments. We propose here that it is useful to define, within the regime of mixed convection, a sub-regime of 'weakly forced convection' in which, to a first approximation, the heat flux is determined by temperature differentials as in free convection and the momentum flux by a perturbation, linear in wind, on free convection. It is further proposed that this regime is governed by velocity scales determined by the heat flux (rather than by the friction velocity as in classical turbulent boundary layer theory). Three candidates for the heat-flux velocity scale are considered; novel definitions of the drag and heat exchange coefficients, based on the preferred scale, are found to show very weak dependence on wind speed up to values of about 5–10 m s^{-1}; but there is some evidence that the usefulness of heat-flux scaling may extend beyond the velocity limits where pure free-convection scaling for heat flux is valid.

1. Introduction

A large number of turbulent shear flows in nature as well as in technology are strongly affected by stratification. In particular, flows in both the oceans and the atmosphere are stratified due to temperature and/or admixture (salinity or humidity) gradients. (In the rest of this paper we restrict our attention to temperature gradients.) The most widely used approach for taking into account the effect of such stratification on a turbulent boundary layer is based on Monin–Obukhov (M–O) similarity theory. This theory has been extensively discussed in both the fluid-dynamical and meteorological literature (Monin 1970; Businger *et al.* 1971; Haugen 1973; Monin & Yaglom 1975; Stull 1988 etc.). The key parameter in the theory is the Obukhov length L, on the basis of which different stability regimes are identified in terms of the ratio $\zeta = z/L$ where z is height above the surface and

$$L \equiv \frac{C_p \rho_0 u_*^3}{k \beta Q_s} = \frac{u_*^3}{k g \alpha \overline{w'T'}};$$

(1.1)

here ρ_0 is a mean or standard density, C_p is the specific heat at constant pressure, u_* is the friction velocity, k is the Kármán constant, β is the buoyancy parameter (= acceleration due to gravity g times the thermal expansion coefficient α) and Q_s the (sensible) heat flux ($= \rho_0 C_p \overline{w'T'}$ where w' is the vertical velocity fluctuation, T' the temperature fluctuation, and the overbar denotes a time mean).

It is well known that z/L is related to the local gradient Richardson number (see e.g. Haugen 1973). The M–O theory has in general received extensive support from field observations, and is widely used in atmospheric and ocean modelling. However, there has been much discussion about the place of M–O theory in the limit of free convection. (See e.g. the contributions of Businger 1973 and Tennekes 1973 in Haugen 1973). In general the observed bulk aerodynamic coefficients increase as wind speed falls, as noted by Bradley, Coppin & Godfrey (1991) from measurements over the West Pacific, and by Rao, Narasimha & Prabhu (1996a, b) from measurements over land. As the latter references point out, the observed fluxes at low winds are much higher than predicted by the well-known Businger relations for M–O theory.

Indeed, the problem of low-wind fluxes has been of great meteorological interest for some time, following the finding of Miller, Beljaars & Palmer (1992) that simulations of tropical climate (including in particular the Indian monsoons) are substantially better with an enhancement of low-wind fluxes over the values given by parameterization schemes earlier in use at the European Centre for Medium-range Weather Forecasts. One common practice of atmospheric modellers to take account of low-wind conditions has been to introduce a 'gustiness' parameter, which replaces the low surface winds generated in the models by some specified higher value (usually in the range 1–3 m s^{-1}: see Hack *et al.* 1993), and continues to use M–O theory at the specified cut-off velocity. Godfrey & Beljaars (1991), who introduced the concept of gustiness, proposed including, as an additional component of wind in the bulk transfer laws for the surface layer, a multiple of the Deardorff free-convection velocity (Deardorff 1972),

$$w_* = \left(\frac{gZ_i}{\theta_v} \overline{w'\theta_v'} \right)^{1/3}, \tag{1.2}$$

where Z_i is the height of the capping inversion in the mixed layer, θ_v is the virtual potential temperature averaged between the mixed layer and *skin*, and θ_v' is the fluctuation in the virtual temperature. Beljaars (1994) used this concept to propose an extension of M–O theory to nearly windless free convection.

Stull (1994) has proposed a different convective transport theory to parameterize the fluxes in the free-convection limit in terms of the mean characteristics of the mixed layer and the surface. He proposes that the fluxes are proportional to (i) an appropriate differential in the relevant mean quantity (temperature, velocity or relative humidity) between the mixed layer and the *skin*, and (ii) a buoyancy velocity scale defined by

$$w_B = \left[\frac{gZ_i}{\theta_v} \Delta\theta_B \right]^{1/2} \tag{1.3}$$

where $\Delta\theta_B$ is an appropriate virtual temperature differential. It should be noted that w_B has no explicit dependence on the flux itself and can have values as high as 30 m s^{-1} in vigorous convection. It is seen that this proposal, like (1.2), involves the overall boundary layer parameter Z_i; but interestingly, Stull notes that the corresponding expression for the heat flux is relatively insensitive to measurement errors of Z_i.

The chief purpose of this study is to present an analysis of atmospheric data which shows that the fluid dynamics of low-wind eddy fluxes in the atmosphere is best seen as part of the regime called mixed convection (see e.g. Kays & Crawford 1993; Gebhart 1971), which spans the range between the two limits of forced and free convection. In the former (latter) buoyancy forces are small (large) compared to inertia forces; the Richardson number is small (negatively large). Within the mixed convection regime, we wish to identify here a subregime that is close to free convection but with low winds; we call this nearly free or (preferably) 'weakly forced'. The present view is similar to but extends that implicitly taken in a penetrating analysis by Grachev (1990). Grachev's analysis made explicit appeal to turbulence models. The present view produces meaningful scaling laws for heat and momentum fluxes without explicitly invoking any turbulence model. The main contributions of the present study are therefore (*a*) the demonstration that the ad-hoc procedures now being followed in geophysical models to parameterize low-wind eddy fluxes can be replaced through the use of a new heat-flux velocity scale that plays the same conceptual role in flows dominated by thermal convection as the friction velocity does in nearly neutral flows; and (*b*) the presentation of the first evidence from atmospheric data showing the organizing power of the new scales, without appealing to specfic turbulence models, e.g. those assuming gradient diffusion in some form, which have for long been subject to the legitimate criticism of making assumptions that are patently unjustified.

2. Background

The problem of estimating surface heat flux in turbulent convection in the absence of an overall (superposed) mean flow (which we shall refer to as 'wind') has a long history (Prandtl 1932; Townsend 1964; Deardorff 1972; Businger 1973). Thus, Townsend (1964) writes the surface heat flux in free convection in the form

$$Q_s = C_s \rho_0 C_p \left(\frac{g}{\theta} \frac{\kappa^2}{\nu} \right)^{1/3} (\Delta\theta)^{4/3}, \qquad (2.1)$$

where κ is the molecular thermal diffusivity, ν the kinematic viscosity and $\Delta\theta$ the difference in potential temperature between the surface and the mixed layer. C_s is a constant whose value was estimated to be 0.2 by Townsend (1964), and as lying in the range 0.1 to 0.24 by Deardorff & Willis (1985). Equation (2.1) is equivalent to the heat flux relation $Nu \sim Ra^{1/3}$ in terms of the Nusselt (Nu) and Rayleigh (Ra) numbers, generally considered appropriate for smooth surfaces.

Niemela *et al.* (2000) have recently carried out experiments in a helium apparatus at ultra-high Rayleigh numbers (going up to 10^{17}, approaching values encountered in the atmosphere), and find that the data are best fitted by the relation $Nu \sim Ra^{0.31}$, which is close to (2.1).

Recently Rao *et al.* (1996*a*, *b*) have shown that atmospheric observations over land during the experiment known as MONTBLEX-90 (Goel & Srivastav 1990; Sikka & Narasimha 1995; a detailed account is available in Narasimha, Sikka & Prabhu 1997) reveal a rapid rise in drag as well as heat exchange coefficient at low winds (although at different rates). While at higher winds there is good agreement between M–O theory and observations, at low winds there is substantial disagreement (amounting to as much as 30 % in the friction velocity u_* and friction temperature θ_*, for example, as may be seen from figure 4*a*, *c* of Rao *et al.* 1996*a*). This shows that M–O theory

(with the Businger relations) is inadequate in the pure free-convection limit (no mean cross-wind).

In particular, Rao *et al.* (1996*b*) have shown that the sensible heat flux measurements made during MONTBLEX-90 obey free-convection scaling fairly well, being on the whole consistent with a 4/3 power law on an appropriate temperature differential, as in (2.1). It was further shown that the (dimensional) drag depends almost linearly on wind speed, but the implications of these findings for similarity theory were not discussed. Since their study, Kondo & Ishida (1997) have also reported a similar 4/3 power law for the sensible heat flux in laboratory experiments in natural convection as well as at low winds in the field. Wind tunnel experiments reported in the engineering literature (see Raju & Narasimha 2003) also provide data that show that the free-convection law is valid up to a limiting (cross-) flow velocity, which they express through a criterion on the value of an internal Froude number.

There have been two precursors of the present results not generally recognized in the meteorological literature, including in our own earlier work referred to above (and kindly brought to our attention by a referee). The first is an ingenious experiment by Ingersoll (1966) on thermal convection between two horizontal disks when the upper disk rotates about a vertical axis – an arrangement which imposes a shear flow on the convection. Ingersoll was able to show that the torque on the lower stationary disk varied linearly with the speed of rotation. It was also found that while there was a discernible effect of rotation on the Nusselt number, it was generally not more than 5–6 %. These results are very significant, although the experimental arrangement provides for a mean velocity that varies linearly with distance from the axis, and does not of course reproduce the kind of conditions that generally prevail in the atmosphere.

The second set of studies is due to Grachev (1989, 1990). In the 1989 paper Grachev used a closure of the turbulent equations to study convection in three layers, including a molecular heat transfer sublayer, a buffer zone, and a zone of developed turbulence. Grachev (1990) is closer to the present concerns. It examines conditions of severe instability when turbulent energy generation by the velocity shear can be neglected in relation to that by buoyancy forces, and treats the mean velocity as a passive scalar. Using concepts of eddy viscosity and conductivity, Grachev derived interesting results to which we shall return later in this paper. He showed that his model agreed with the laboratory experiments of Ingersoll (1966), Fukui, Kanajima & Ueda (1983) and Komori *et al.* (1982), but considered "an experimental test under full-scale conditions [in the atmosphere] ... difficult". To our knowledge, there is to-date no analysis of observational data in the atmosphere over land that sheds light on the scaling behaviour in this regime, which in our view is most appropriate to designate as weakly forced convection.

In relation to the other proposals discussed in §1, it is interesting to note the comment of Beljaars (1994) that (in spite of the appearance of Z_i in (1.2)) the significant parameter in determining fluxes is the shape of the profiles close to the surface, rather than at $z \gg |L|$. This suggests that a local similarity theory (which would necessarily have to be based on different principles) may still be feasible. Another remarkable finding of Beljaars is that the heat flux results obtained from his M–O type scheme yield values for the Townsend constant C_s that are in the same range as found in laboratory experiments. These findings provide pointers to the present analysis.

3. Observational data analysed

The data analysed here come from two atmospheric experiments. For the MONTBLEX data, Rudrakumar, Ameenullah & Prabhu (1995) present a detailed description of the tower instrumentation, the associated data acquisition system and the various quality checks adopted to ensure the reliability of acquired data. (We shall consider the accuracy of the data shortly.) The sensors providing the data were mounted on a 30 m high guyed uniform triangular lattice structure, with booms fitted at 6 levels (1, 2, 4, 8, 15, 30 m above the surface). Horizontal arms were attached to these booms at a distance of about 1.3 m from the body of the tower. The booms could be partially rotated about the vertical and horizontal axes to facilitate orientation of the sensors towards the general direction of the prevailing wind and to ensure that the instrument posts are horizontal.

The data used in the present analysis were acquired at Jodhpur (26°18′N, 73°04′E) over a period extending from 9 June to 20 August 1990. The sonic anemometer (model SWS-211/3KE, made by Applied Technologies Inc., USA) was placed at a height of 4 m above the surface, the cup anemometers at six heights namely 1, 2, 4, 8, 15 and 30 m, and the platinum wire resistance thermometers at the four heights 1, 8, 15 and 30 m. The sonic anemometer provides wind and virtual temperature fluctuations to a frequency response of 8 Hz at hourly intervals during intensive observation periods (Srivastav 1995), otherwise at three-hourly intervals continuously for 10 min (15 min) from 15 June to 7 July (6–14 June and 8 July–20 August). The total number of data sets acquired during the period was 676.

It is well known that the accuracy of measured vertical velocities, and hence also of the eddy fluxes obtained by the direct correlation technique, depends on the accurate alignment in the vertical of the associated velocity sensors. The alignment was ensured by a plumb bob that hung over the whole length of the tower. The use of a guyed mast with an open triangular lattice structure (of approximately 40 cm side), and the length of the instrument-carrying boom (extending 1.3 m from the body of the tower), kept flow distortion due to the tower very low. (See pictures of tower and boom in Narasimha *et al.* 1997.) The quality of the data is demonstrated by the excellent agreement between sonic and propeller anemometer velocities, and between the value of σ_w (r.m.s. fluctuation of the vertical velocity) measured in the present experiments and elsewhere under near-neutral conditions (Rudrakumar *et al.* 1995). Thus, the momentum function ϕ_m from the present measurements lies within the range given by various earlier authors (Rao *et al.* 1996b); and the temperature function ϕ_θ shows close agreement with Businger's formulation (Rao 2004). For all these reasons the MONTBLEX data analysed here can be considered reliable.

The tower was installed in a farm field, which at the time of the observations reported here was covered with small pebbles or patches of grass. A detailed description of the tower site, including estimates of roughness length and description of prevailing weather, is given by Rao (1996).

The prevailing direction of the wind at the tower was between southeast and west. The momentum roughness length was estimated at an average value of 1.23 cm in the sector between 200° to 230°, which was relatively flat with no obstacles on the ground; this sector will be called the 'smooth' sector in the following. In the rest of the site covered by the prevailing wind directions the roughness length was somewhat higher, at an average value of 4.5 cm; this will be called the 'rough' sector. For estimating the temperature at the surface required in some of the correlations below, the thermal roughness height was taken as one order smaller than these values, as recommended by Garratt (1978).

During the observation period u_* occasionally reached a value of about $0.7\,\mathrm{m\,s^{-1}}$ (being generally lower), z/L varied from -2.5 to $+0.5$ and sensible heat flux went up to $400\,\mathrm{W\,m^{-2}}$.

Important supplementary data come from the boundary layer field experiment BLX83 carried out between 26 May and 18 June 1983 near Chickasha, Oklahoma ($35°02'$N, $97°51'$N) using the NCAR aircraft Queenair (Stull 1994). The terrain was generally flat, with average roughness length of 5 cm. As 24 out of the 28 data points are characterized by wind speeds less than $10\,\mathrm{m\,s^{-1}}$ under highly unstable conditions, BLX83 provides some valuable data on the low-wind convective regime. The mixed layer depth (or equivalently, the height of the capping inversion) was defined as the height at which there is a 50–50 mixture of the free atmosphere and mixed layer air, and was obtained from ground-based lidar during scans along the aircraft track. Eddy correlation measurements of heat, moisture and momentum fluxes were made during the near-surface legs of the aircraft track ($0.03 < z/Z_i < 0.1$). Skin parameters were obtained by a downward-looking radiometer and by an NCAR portable Automated Mesonet Station.

4. Assessment of M–O similarity at low winds

Based on M–O theory (assuming it is valid), it is possible to estimate both momentum and sensible heat flux using measured velocity and temperature profiles and appropriate stability functions such as those proposed e.g. by Businger *et al.* (1971). Rao *et al.* (1996a) have done this, after segregating the MONTBLEX data on the basis of the value of the mean velocity at 10 m height, U_{10} ($\gtrless 4\,\mathrm{m\,s^{-1}}$), and of the flux Richardson number R_f. They found that while the high-wind, low-instability data agree well with M–O theory, the low-wind high-instability data (flux Richardson number $R_f < -1.0$) show substantial departures, sometimes amounting to as much as 30 % in the friction velocity u_* (and about 70 % in the drag coefficient).

This can be demonstrated in different ways that are more direct. It must first of all be realized that plots of the classical non-dimensional temperature gradient ϕ_θ of M–O theory, defined as

$$\phi_\theta(\zeta) = \frac{kz}{\theta_*}\frac{\partial \bar{T}}{\partial z}, \quad \theta_* \equiv -\frac{Q_s}{\rho_0 c_p u_*},$$

against the stability parameter $-\zeta \equiv -z/L$, are not sufficiently sensitive tests of the theory. The data presented by Businger *et al.* (1971) seem in slightly better agreement with a $(-\zeta)^{-1/2}$ dependence of ϕ_θ for $\zeta \lesssim -0.8$ (whereas pure free convection would require a $(-\zeta)^{-1/3}$ dependence), but while the differences in such a plot do not appear marked, flux values can be significantly different. The point we are making can be seen through a direct comparison of observed and theoretically estimated fluxes. To do this, we first estimate the eddy fluxes from M–O theory, and compare them with observations. (The M–O estimates are derived from measured values of velocity and temperature gradients and the similarity functions proposed by Businger *et al.* (1971).) Figure 1 shows that the momentum flux so estimated from M–O theory for MONTBLEX data tends to vary (as may be expected) in proportion to the square of the wind speed, almost all the way up to $U_{10} \sim 8\,\mathrm{m\,s^{-1}}$. We show below (e.g. figure 4) that observations show a different behaviour (see also Rao *et al.* 1996a). The heat flux also shows departures from M–O theory. This is best shown by the analysis of Rao *et al.* (1996b), comparing values of the temperature scale θ_* (defined as $-\overline{w'\theta_v'}/u_*$), as derived from mast profile data using M–O theory, with values measured directly from
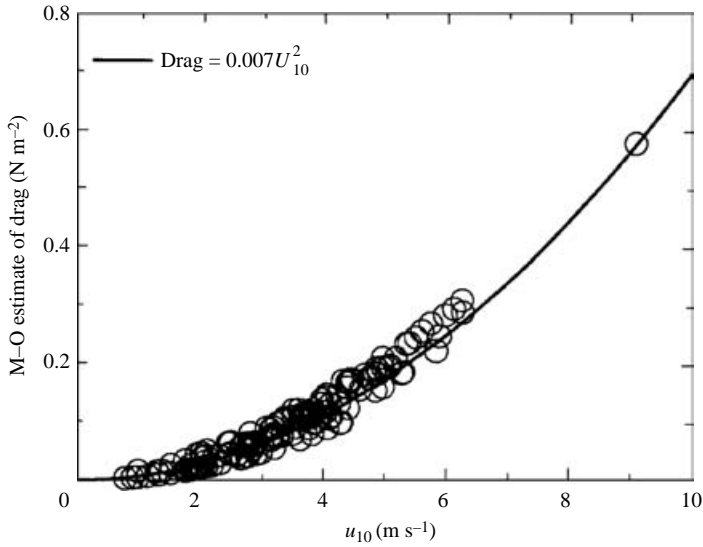
FIGURE 1. Estimates of drag per unit surface area (stress) provided by Monin–Obukhov theory for values of mean velocity and temperature gradient derived from measurements in MONTBLEX-90. Curve shows a least-squares fit to the estimate.
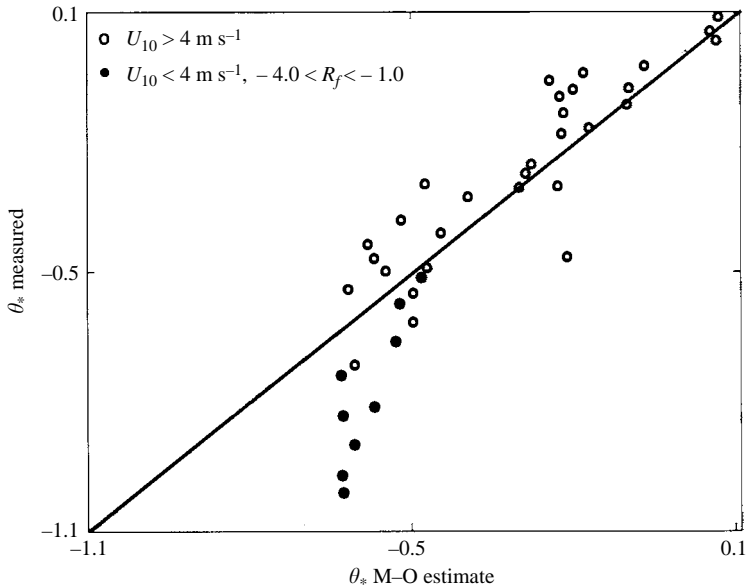
FIGURE 2. Comparison between friction temperature θ_* as derived from mast data using M–O theory (abcissa) and as measured by the eddy correlation technique. Data from MONTBLEX 90, after Rao *et al.* (1996*b*).

the eddy correlation technique. (The profile data are computed assuming an average value for the roughness height at the site.) A part of these results is shown in figure 2; note that the data shown here are selected as they are segregated by wind velocity and flux Richardson number. It is seen that at relatively high winds ($>4\,\mathrm{m\,s^{-1}}$) the

Levels	$Q_s/(\Delta\theta)^{4/3}$ (in W, m, K units)	C_s
1 and 10 m	145	12.3
1 and 30 m	85.0	7.2
z_T and 30 m	25.5	2.17

TABLE 1. Values of coefficient C_s in (2.1), for different temperature differentials.

measured values of θ_* are in close agreement with M–O theory estimates, whereas at wind speeds less than $4\,\mathrm{m\,s^{-1}}$ in highly unstable conditions (flux Richardson numbers between -1.0 and -4.0, ζ less than about -0.5) M–O theory appreciably underestimates the true flux. (We incidentally take this opportunity to point out that some of the axes on figure 4b,d of Rao *et al.* (1996a) are mislabelled; the correct ones, on both abscissa and ordinates, are -0.8 and 0.0 in figure 4b, and -1.2 and -0.2 in figure 4d.)

We now consider each of the fluxes separately.

5. The sensible heat flux

Figure 3(a) shows the heat flux variation with the characteristic temperature differential $\Delta\theta$ taken as the difference between values at $1\,\mathrm{m}$ and $30\,\mathrm{m}$ above the surface, the lowest and highest levels at which data are available from the MONTBLEX tower. (Note that at the relatively small values of z we are considering, the virtual temperature θ is practically identical with the ordinary temperature T.) The data collapse fairly well in the plot of $Q_s^{3/4}$ against $\Delta\theta$, as suggested by (2.1), albeit with some fairly large deviations, especially in the rough sector. The best fit is $Q_s^{3/4} = 29.0(T_1 - T_{30})[\pm 11.6]$ (here and in what follows this notation stands for the best fit $[\pm$ the root mean square deviation]), and the correlation coefficient is 0.88 [0.82–0.93] (the numbers in square brackets indicating the 95 % confidence interval as determined by Student's t-test). There is some indication that the heat flux is slightly different between the rough and smooth sectors, the best fits being

$$Q_s^{3/4} = 28.0(T_1 - T_{30}) \quad [\pm 15.01] \tag{5.1}$$

and

$$Q_s^{3/4} = 30.0(T_1 - T_{30}) \quad [\pm 8.4] \tag{5.2}$$

respectively. Note that the scatter in the smooth sector is about half of that in the rough sector, but the overall heat flux itself is only slightly affected.

The nature of this result is not sensitive to the choice of temperature differential; thus if we take $\Delta\theta = T_{z_T} - T_{30}$, with z_T determined as mentioned in §3, a plot very similar to figure 3(a) (not shown here) is obtained, the best fit being

$$Q_s^{3/4} = 11.0(T_{z_T} - T_{30}) \quad [\pm 24.9]. \tag{5.3}$$

The values of the coefficient C_s for different choices of temperature differential are listed in table 1. Note that because the temperature differentials used here are different from those used by Townsend (1964), Deardorff & Willis (1985) and others, the numerical value of the factor in (5.1)–(5.3), or in table 1, cannot be directly compared with those quoted in these earlier references. It is seen that the general
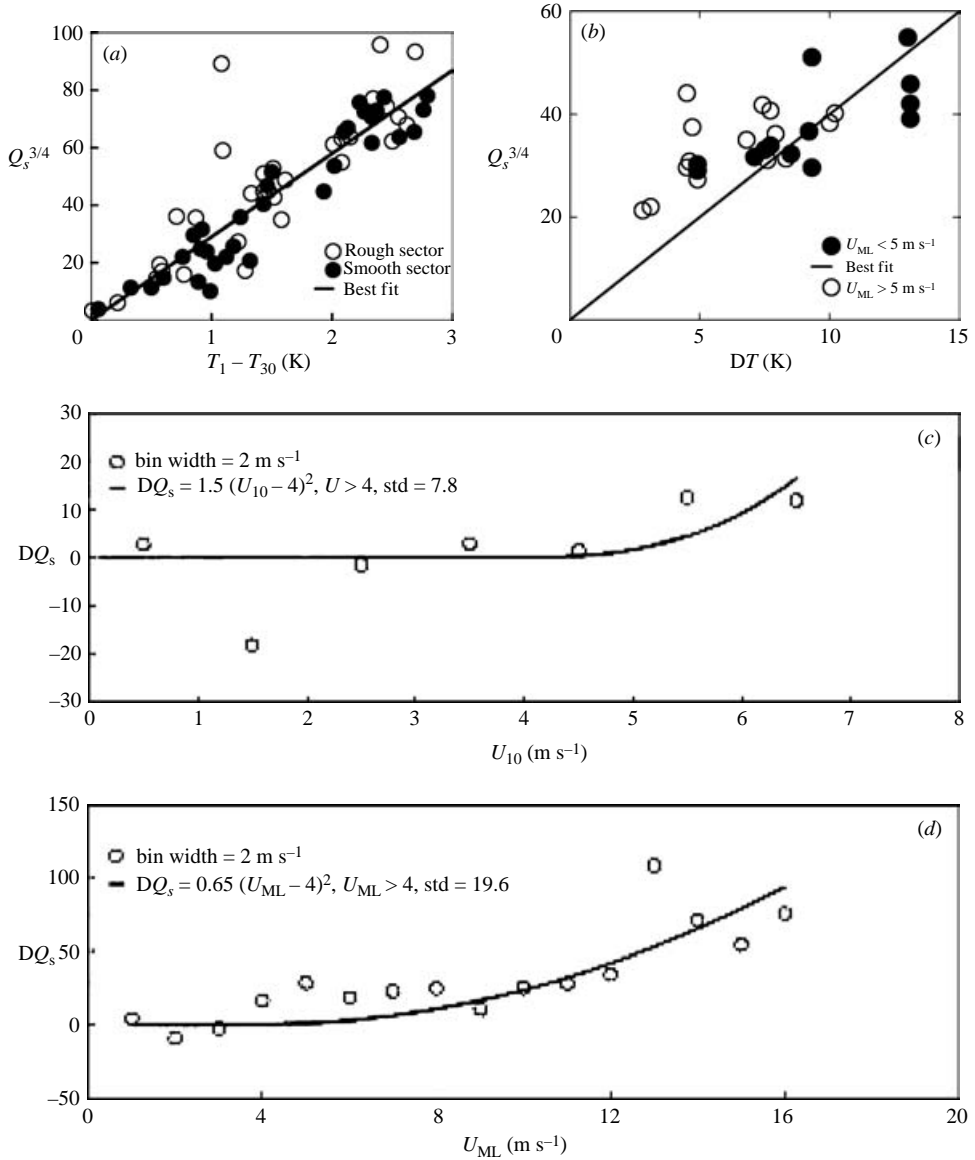
FIGURE 3. Observed sensible heat flux as a function of a characteristic temperature differential, to show the range of a 4/3 power dependence. (*a*) Data from MONTBLEX. (*b*) Data from BLX83, indicating separately low- and high-wind observations. (*c*, *d*) Deviations of Q_s from best fit as function of wind speed, data from MONTBLEX (*c*) and BLX83 (*d*).

validity of the power law is not dependent on the precise choice of the levels at which the temperature data are obtained, but the scatter could be less with certain choices.

The scatter seen in figure 3(*a*) is appreciably smaller than in other analyses of comparable atmospheric data (see e.g. Miller *et al.* 1992). We shall now show that except at the lowest wind speeds where the heat flux seems to depend solely on the temperature differential, the data suggest a weak higher-order dependence on wind as well. This can be seen in the data from both MONTBLEX and BLX83. The parameters available in the latter data-set are the temperature differential DT between

the skin and the mixed layer, and the mixed layer velocity U_{ML}; these are again not directly comparable to the measurements made as part of MONTBLEX. Points for surface heat flux Q_s are plotted against DT in figure 3(b). It is seen that, while for wind velocities $U_{\mathrm{ML}} < 5\,\mathrm{m\,s^{-1}}$ (filled circles) the 4/3 power law agrees reasonably with the data, at speeds $U_{\mathrm{ML}} > 7.5\,\mathrm{m\,s^{-1}}$ the heat flux at given DT tends to be generally higher.

That the apparent 'scatter' seen in figures 3(a, b) conceals a small but systematic dependence on wind speed can be seen from figures 3(c, d). We plot here the departure of the observed heat flux from the 4/3 power law fit at low winds against wind velocity; each point here represents an average over a bin of width $1.0\,\mathrm{m\,s^{-1}}$ in the MONTBLEX data and $0.5\,\mathrm{m\,s^{-1}}$ in the BLX83 data. The deviations in heat flux are negligible for $U_{10} < 4.5\,\mathrm{m\,s^{-1}}$ (except for the point at $1.5\,\mathrm{m\,s^{-1}}$) and for $U_{\mathrm{ML}} < 6\,\mathrm{m\,s^{-1}}$ respectively in the two data sets; they increase appreciably at higher winds. The total number of points at $U_{10} < 4.5\,\mathrm{m\,s^{-1}}$ in the MONTBLEX data set is about 60 (distributed among 5 bins), and at $U_{ML} < 6\,\mathrm{m\,s^{-1}}$ in the BLX83 data set is about 14 (distributed among 6 bins).

This conclusion, that the free-convection law for heat flux is applicable even in situations with limited cross-wind velocities, is in agreement with the trend of laboratory data on heat flux analysed by Raju & Narasimha (2003). By a reanalysis of published data on mixed-convection heat transfer rates on cylinders, spheres and flat plates, they find that, up to a fairly well-defined value of the cross-wind velocity, the measured Nusselt numbers (Nu) are very close to natural-convection values. The critical cross-wind velocity is best expressed in terms of an internal Froude number

$$Fr = U[g\ell\Delta T/T_r]^{-1/2},$$

where ℓ is a length scale characteristic of the surface in the flow, ΔT is a characteristic temperature difference and T_r is a reference temperature. In each of the three flows they find that data show good collapse in the plane of Nu vs. Fr, and that the free-convection heat transfer law is valid to within 5% as long as Fr is below a critical value that depends on body geometry.

We therefore conclude that the heat flux remains independent of wind speed at sufficiently low winds, and is determined (to the lowest order) by temperature differences as in free convection; as the wind speed increases beyond a certain limiting value defined by a Froude number there is a systematic deviation from the free-convection law. We shall return to this issue in §9, but note here that both laboratory and atmospheric data point to the existence of this sub-regime of what we have called weakly forced convection within the much broader regime of mixed convection.

6. The momentum flux

The momentum flux, computed by the eddy correlation technique as $-\rho\overline{U'w'}$, where U' is the fluctuation in the horizontal wind speed along the mean wind direction, is shown as a function of wind speed U_{10} in figure 4(a), for points from the smooth sector in the MONTBLEX data set. It is seen that, in contrast to figure 1, the drag varies linearly with wind speed ($0.047U_{10}$ [±0.089]) to a very good approximation, certainly up to wind speeds of about $5\,\mathrm{m\,s^{-1}}$ (the correlation coefficient is 0.79 [0.69–0.86]). (The corresponding relation is $0.051U_{10}$ [±0.10] in the rough sector and $0.050U_{10}$ [±0.097] overall: the drag is slightly higher in the rough sector. Note that we use the word 'drag' to denote drag per unit surface area, i.e. it is equivalent to stress or momentum
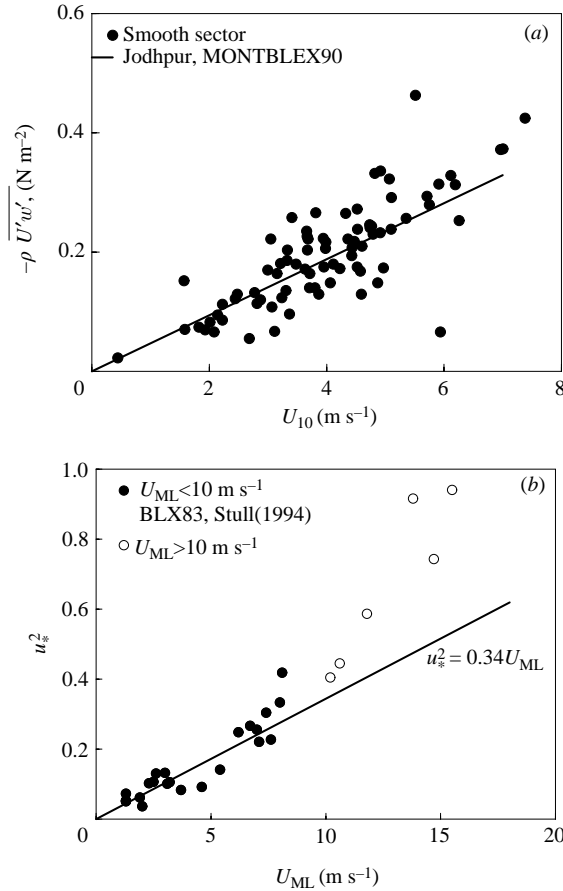
FIGURE 4. Observed drag as function of wind speed. (*a*) Data from MONTBLEX, (*b*) data from BLX83. In (*b*) the linear expression is a fit only to observations with $U_{ML} < 10\,\mathrm{m\,s^{-1}}$ (i.e. filled circles).

flux.) By comparison with figure 1 it is also clear that virtually all the measured flux values lie above the M–O prediction curve. Indeed, the momentum flux, and consequently the drag, does not follow M–O theory but is instead proportional to the first power of U_{10} – i.e. (as already pointed out by Rao *et al.* 1996*a*), the drag coefficient $C_D (\equiv \overline{U'w'}/U_{10}^2) \sim U_{10}^{-1}$ to a first approximation – a result noted by Grachev (1990) also.

Figure 4(*b*) shows the BLX83 data. We can see here that the drag (proportional to u_*^2) increases linearly with U_{ML} up to $U_{ML} \simeq 8\,\mathrm{m\,s^{-1}}$; at higher wind speeds the drag increases more rapidly, as may be expected from M–O theory.

Taken together with the result for heat flux shown in figure 3, these results indicate that wind is acting as a small perturbation to the free-convection regime, producing a small higher-order effect on the heat flux and generating a first-order momentum flux as a departure from a pure free-convection regime where the net drag (as a suitable spatial or ensemble average, see §9) vanishes at zero wind, i.e. in the absence of a mean cross-flow velocity.

Furthermore, the measured heat flux shows no systematic variation with measured momentum flux (Rao 2004).

We note that the wind velocity at which heat flux deviates from the free-convection law ($U_{10} \simeq 5\,\mathrm{m\,s^{-1}}$ in MONTBLEX-90, $U_{\mathrm{ML}} \sim 8\,\mathrm{m\,s^{-1}}$ in BLX83; see figure 3c, d) is about the same as the value at which drag departs from a linear dependence on wind speed (figure 4a, b). This finding reinforces the present concept that the flow regime below these limiting velocities may be considered to define a sub-regime of 'weakly forced' convection within the much broader regime of mixed convection. At wind velocities beyond these values we still have a mixed convection regime.

We can ask whether the weakly forced regime is defined by a value for the Deardorff velocity scale w_*, given by (1.2). The MONTBLEX data do not have simultaneous measurements of Z_i and heat flux, so precise estimates of w_* cannot be made. However, sodar and radio sonde measurements (Gera et al. 1996; Rajkumar et al. 1996) indicate that Z_i was generally less than 900 m, but other data tabulated by the latter sometimes indicate a value of Z_i of several thousand metres. If we take $Z_i \simeq 1000\,\mathrm{m}$ we find that w_* varies in the range 1.4 to $2.8\,\mathrm{m\,s^{-1}}$, and with $Z_i = 2000\,\mathrm{m}$ the range goes up to 2–$3\,\mathrm{m\,s^{-1}}$. This may be compared with the results shown in figure 3(c), which suggests that the heat flux remains close to the free-convection law for $U_{10} \lesssim 4.5\,\mathrm{m\,s^{-1}}$.

Another criterion is provided by the departure of measured θ_* from M–O estimates, shown in figure 2. Based on a reanalysis of the data presented in Rao et al. (1996a), this departure is found to begin from $z/L \lesssim -0.5$, which may be taken as another indicator of the prevalence of free-convection heat flux. These findings suggest the analysis of the following sections.

7. Grachev's approach

Before presenting the data it is worthwhile to briefly describe Grachev's approach. Grachev (1989) first derives the temperature profile in free turbulent convection by dividing the whole domain into three layers following Kraichnan (1962), and using the Prandtl–Kolmogorov K–L model. He finds that the theoretical profiles are in good agreement with laboratory data.

In a sequel, Grachev (1990) studies the friction law in the free-convection limit, assuming that the mean velocity can be treated as a passive scalar. Using similarity arguments he derives a result for the drag in the form

$$u_*^2 = A_u U (\beta \nu H)^{1/4} \tag{7.1}$$

where u_* is the friction velocity, A_u a constant, U the velocity as $z \to \infty$, and $H = Q/\rho_0 C_p$ the kinematic heat flux; the quantity $(\beta \nu H)^{1/4}$ has the dimensions of velocity, and will be called here the Grachev velocity scale U^{G}. Equivalently, the result can be expressed in terms of the Ingersoll number, which Grachev defines as

$$In \equiv \frac{u_*^2 d}{\nu U}$$

where d (in the case of convection between parallel plates) is half the separation distance between the plates. Equation (7.1) can then be rewritten as

$$In = A_u \left(\frac{Ra\,Nu}{Pr^2} \right)^{1/4} \equiv A_u Gr^{1/4},$$

where Gr is the flux Grashof number. Detailed velocity profiles are also derived, again by use of a Prandtl–Kolmogorov model. Comparison with the laboratory experiments of Ingersoll (1966) for the torque, and of Townsend (1972), Fukui et al. (1983) and

Komori *et al.* (1982) for the velocity profile, are found to show good agreement. Grachev considers the possibility of testing his theory against data on the momentum flux between the air and ocean under conditions of strong instability of the surface air layer, but concludes that such a test is difficult due to the directional irregularity of the mean wind at low wind speeds. (We shall however find it is otherwise in the atmosphere.)

8. The present approach: new velocity scales

The results of §§4–7 strongly suggest that eddy fluxes at low winds are best seen as constituting a distinct thermal flow regime of weakly forced convection. We propose that in this regime, which in the limit has $u_* \to 0$, $\overline{U'w'} \to 0$ but $\overline{w'T'} \nrightarrow 0$, the scaling is driven primarily by the non-vanishing surface heat flux Q_s.

Using the heat flux as the primary variable (and not the drag, as in M–O theory), two new velocity scales may be defined respectively as

$$\hat{U} = \frac{Q_s}{\rho_0 c_p \Delta\theta} \tag{8.1}$$

and

$$\hat{\hat{U}} = \frac{\overline{T}^{1/3}}{\rho_0 c_p} \frac{Q_s}{(\Delta\theta)^{4/3}} = \hat{U}\,(\Delta\theta/\overline{T})^{-1/3}, \tag{8.2}$$

where $\overline{T}$ is a suitable average temperature. The velocity scale $\hat{U}$ may be seen as a measure of the vertical velocity that generates the heat flux Q_s. The second velocity scale $\hat{\hat{U}}$ differs from the first by the factor $(\overline{T}/\Delta\theta)^{1/3}$, inspired by the 4/3 power law for the heat flux expressed by equation (2.1).

The relations between these velocity scales are easily written down *if we can assume that the heat flux is given by the free-convection formula* (2.1). Noting that $\beta = g/\theta$, and substituting from (2.1), we find

$$U^{\mathrm{G}} \equiv (\beta\nu H)^{1/4} = C_s^{1/4} Pr^{-1/6}(g\nu)^{1/3}(\Delta\theta/\theta)^{1/3}, \tag{8.3}$$

$$\hat{U} = C_s Pr^{-2/3}(g\nu)^{1/3}(\Delta\theta/\theta)^{1/3}$$
$$= C_s^{3/4} Pr^{-1/2} U^{\mathrm{G}}, \tag{8.4}$$

and

$$\hat{\hat{U}} = C_s Pr^{-2/3}(g\nu)^{1/3}. \tag{8.5}$$

It is important to note, however, that to the extent that the actual heat flux may depart from (2.1) as wind increases (as indicated in figure 3*c*, *d*), the relations given above will cease to hold.

Figure 5 displays the velocity scales we are discussing. Figure 5(*a*, *b*) shows $\hat{U}, \hat{\hat{U}}$ for the MONTBLEX data as a function of U_{10}. According to (8.5) $\hat{\hat{U}}$ should be a constant in pure free convection; figure 5(*b*) suggests that there might be a weak increasing trend with U_{10}. Figure 5(*c*) shows $\hat{U}$ for the BLX83 data as a function of U_{ML}, and again there is a weak increasing tendency with wind speed. Figure 5(*d*, *e*) shows the Grachev velocity scale as a function of the present proposed scales. It is seen that U^{G} does show an approximately linear increase with $\hat{U}$, of the kind that may be expected from (8.4), but only up to $\hat{U} \sim 0.1\,\mathrm{m\,s^{-1}}$. The value of U^{G} hardly changes as $\hat{\hat{U}}$ increases to $0.3\,\mathrm{m\,s^{-1}}$. The correlation of U^{G} with $\hat{\hat{U}}$ is similar but weaker.

We shall find below that both the scales $\hat{U}$ and $\hat{\hat{U}}$ may have their uses.
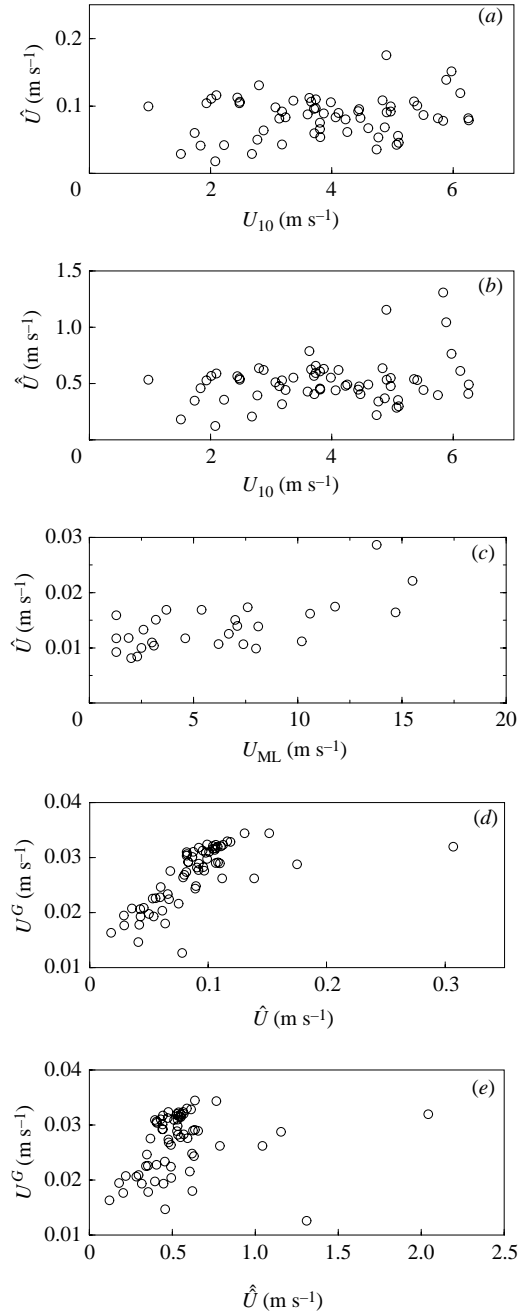
FIGURE 5. Different velocity scales compared. (*a*, *b*) MONTBLEX data; (*c*) BLX83 data, showing the heat-flux velocity scales proposed here as function of wind speed; (*d*, *e*) Grachev's velocity scale compared with present proposals.

It is immediately seen that a modified heat exchange coefficient, defined as

$$\hat{C}_H = \frac{Q_s}{\rho_0 C_p \hat{U} \Delta \theta}, \tag{8.6}$$
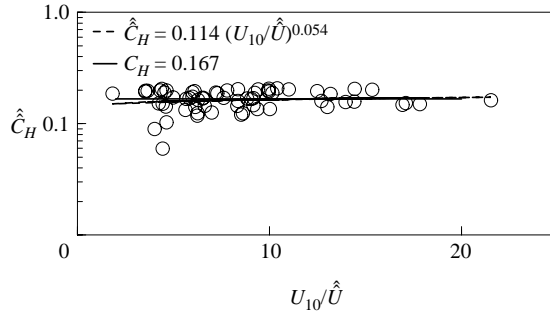
FIGURE 6. Heat transfer coefficient $\hat{\hat{C}}_H$, as proposed here, does not vary significantly with wind speed, but a best-fit power law to MONTBLEX data indicates an exponent of 0.054.

will, by definition, be unity independent of wind speed. Even a coefficient defined as

$$\hat{\hat{C}}_H = \frac{Q_s}{\rho_0 C_p \hat{\hat{U}} \Delta\theta} \tag{8.7}$$

is nearly constant (figure 6), but on closer examination reveals a slow variation with wind speed, given by the relation

$$\hat{\hat{C}}_H = 0.114(U_{10}/\hat{U})^{0.054}.$$

Equations (8.3)–(8.5) may be seen as establishing a connection between the present heat-flux velocity scales and an intrinsic viscous–gravity velocity scale when heat transfer is given by free convection: at fixed Prandtl number $\hat{U} \propto (g\nu)^{1/3}$ in this limit. We retain $U^{\hat{}}$ as a heat-flux velocity scale that turns out to be of value even when the heat flux is not strictly given by (2.1) but has the weak dependence on wind shown in figure 3(c, d).

There is a suggestion in the data that the 4/3-power law of (2.1) may be more closely obeyed when the temperature differential $\Delta\theta$ corresponds to near-surface values, rather than (say) skin and mixed-layer levels. On the other hand it is likely that the air temperature T_1, at a height of 1 m above ground, gives better results than the ground or skin temperature T_g, which in reality can be far more spatially non-homogeneous than the more robust T_1, but these suggestions need to be tested in greater detail by special field measurement campaigns.

We now introduce three new candidates for a definition of the drag coefficient,

$$\hat{C}_D = \frac{D}{\rho_0 \hat{U} U_0}, \quad \hat{\hat{C}}_D = \frac{D}{\rho_0 \hat{\hat{U}} U_0}, \quad C_D^G = \frac{D}{\rho_0 U^G U_0}, \tag{8.8}$$

where $D = -\rho_0 \overline{U'w'}$ represents drag and U_0 is a characteristic wind velocity, equal to U_{10} in the MONTBLEX measurements and U_{ML} in BLX83. These definitions incorporate the observed linear dependence on wind, and utilize the heat-flux velocity scales proposed here for non-dimensionalization. Figure 7(a–d) shows the variation of the newly defined drag coefficients with the appropriately non-dimensionalized wind speed, for both MONTBLEX and BLX83 data. In presenting MONTBLEX data, we have rejected measurements for which $\Delta\theta < 0.05°C$; such a threshold is based on the limited accuracy of the temperature data, and is within the noise level of the measurements. From figure 7(a, b) we see that the drag coefficients show a slow rise
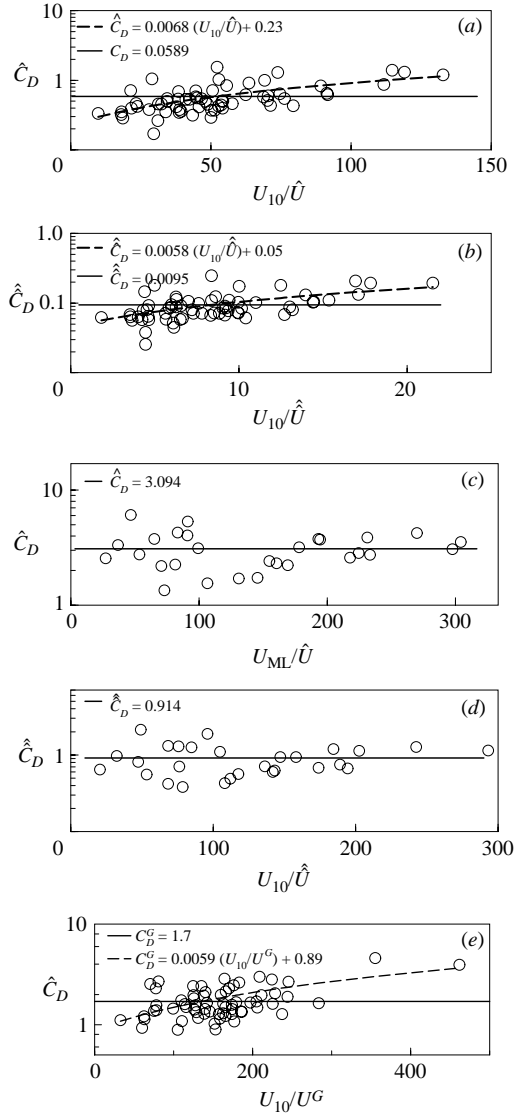
FIGURE 7. Drag coefficients. (*a*, *b*) MONTBLEX data, present scaling. (*c*, *d*) BLX83 data, $U_{\mathrm{ML}} < 10\,\mathrm{m\,s^{-1}}$, present scaling. (*e*) MONTBLEX data, Grachev scaling.

with wind speed,

$$\hat{C}_D \simeq 0.23 + 0.0068(U_{10}/\hat{U}) \quad [\pm 0.29], \qquad \hat{\hat{C}}_D = 0.05 + 0.0058(U_{10}/\hat{\hat{U}}) \quad [\pm 0.04].$$

(The corresponding correlation coefficients are 0.60[0.42–0.74] and 0.54[0.33–0.69].) For the BLX83 data there is hardly any variation with wind speed, and we can write

$$\hat{C}_D = 3.09 \quad [\pm 1.1], \qquad \hat{\hat{C}}_D = 0.914 \quad [\pm 0.424].$$

Figure 7(*e*) shows the drag normalized using the Grachev scale. The best fit is

$$C_D^{\mathrm{G}} = 0.0059 + 0.89(U_{10}/U^G) \quad [\pm 0.58].$$

Levels	$\hat{C}_D$	$\hat{\hat{C}}_D$
1 and 10 m	0.388	0.057
1 and 30 m	0.589	0.095
z_T and 30 m	1.562	0.345

TABLE 2. Values of drag coefficient defined in present work, using different temperature differentials for defining heat-flux velocity scale.

The weaker wind dependence and lower scatter of $\hat{C}_D$ and $\hat{\hat{C}}_D$ suggest that the new velocity scales (8.1) and (8.2) are the most appropriate for drag parameterization. The scaling is effective for both smooth and rough sectors.

The near-independence of $\hat{C}_D$ and $\hat{\hat{C}}_D$ of wind speed is preserved irrespective of the temperature differential used in the definition of the velocity scale; the actual values of the coefficients however depend on the choice of ΔT. Table 2 shows the values obtained from an analysis of MONTBLEX data for three such choices, namely the differential between 1 and 10 m, 1 and 30 m and z_T and 30 m respectively.

It is seen that the range of wind speed over which the weakly forced convection regime prevails, as determined from the drag, extends at least up to $U_{10}/\hat{U} \lesssim 18$ or $U_{\mathrm{ML}}/\hat{U} \lesssim 300$.

It should be pointed out that the above approach for analysing momentum flux may be applicable only over land. The reason is that, over sea, convection at low winds may be accompanied by ocean swell, which could result in upward momentum flux or negative drag (see e.g. Grachev & Fairall 2001).

9. A model-free approach to the low-wind limit

In §7 we described briefly Grachev's (1990) approach to convection in the presence of wind. We present below a perturbation approach to the problem intended to provide a brief explanation of the observed behaviour of both momentum and sensible heat fluxes. The explanation is general in the sense that it does not appeal to any specific turbulence model.

We may begin with the momentum flux. The fluctuating velocity field may be expanded in a small parameter ϵ (to be identified below) that characterizes the low-wind limit:

$$U' = U'_0 + \epsilon U'_1 + \cdots, \quad w' = w'_0 + \epsilon w'_1 + \cdots, \tag{9.1}$$

so that

$$\overline{U'w'} = \overline{U'_0 w'_0} + \epsilon(\overline{U'_1 w'_0} + \overline{U'_0 w'_1}) + O(\epsilon^2). \tag{9.2}$$

In pure free convection (with no cross-wind), neither U'_0 nor w'_0 will vanish, nor even the time average $\overline{U'_0 w'_0}$ at a particular station relative to a given convection system such as e.g. a plume. (Indeed there are theories, such as the one proposed by Schumann (1988), that attempt to deduce the character of free convection using ideas of forced convection locally for such time-averages.) However, an appropriate spatial or ensemble average (denoted by angular brackets), $\langle U'_0 w'_0 \rangle$, must vanish at no wind, for reasons of symmetry: the associated Reynolds stresses will have different directions at different points but will have to add vectorially to a sum of zero. Furthermore turbulent free convection is characterized by the intermittent

break-away, from the hot surface, of thermals or plumes that wander about the surface (Townsend 1959; Turner 1973). It thus follows that we can write, to $O(\epsilon^2)$,

$$\langle \overline{U'w'} \rangle = \epsilon \langle (\overline{U_1'w_0'} + \overline{U_0'w_1'}) \rangle, \tag{9.3}$$

which will in general be proportional to a free-stream velocity such as U_{10} through U_1' and w_1', which again can have components that correlate with w_0' and U_0'. This provides a plausible explanation for the linear increase in drag with wind speed displayed in figure 4, and, in the present limit of weakly forced convection, is analogous to Grachev's argument that wind acts as a passive scalar.

Making a similar expansion for the heat flux we may write

$$\langle \overline{w'T'} \rangle = \langle \overline{w_0'T_0'} \rangle + \epsilon \langle (\overline{w_0'T_1'} + \overline{w_1'T_0'}) \rangle + O(\epsilon^2), \tag{9.4}$$

the difference from the momentum flux being that the first term on the right of (9.4) definitely does not vanish, being proportional to the free-convection heat flux. Because of the presence of T_1' and w_1', the term of $O(\epsilon)$ in (9.4) represents in general a contribution linear in U_{10}, which is a measure of the strength of the perturbation produced by cross-wind. However, preliminary analysis of data on heat flux presented in §5 suggests that, at sufficiently low wind speeds, an $O(\epsilon)$ term linear in U_{10} may not be present. This is plausible, for the following reason. In the standard equation for the temperature field, the additional term that appears in the presence of wind, beyond those that describe free convection, is the contribution of horizontal advection, which in standard notation may be written

$$\bar{u}\frac{\partial \bar{T}}{\partial x} + \bar{v}\frac{\partial \bar{T}}{\partial y} \tag{9.5}$$

(the vertical advection is present even in free convection). Now if the horizontal velocity is small, and the horizontal gradient of temperature is also small – as it tends to be of order $10^{-5}\,\mathrm{K\,m^{-1}}$ or less in the tropics (as long as the terrain is not highly non-homogeneous) – the term (9.5) will indeed tend to be of higher order. This provides a plausible explanation for why the 4/3 power law (2.1) seems to be valid even at velocities as high as $5\,\mathrm{m\,s^{-1}}$ or more.

We now identify a quantitative expression for ϵ. Following the discussion in §8, we may take for ϵ a measure of the vertical component w_τ of a shear-induced velocity relative to a characteristic convective velocity $\hat{w}$. Extrapolating from standard turbulent boundary layer similarity laws it is reasonable to take $w_\tau \propto u_*$, the friction velocity, which itself is typically of the order of 5% of U_{10}. In vigorous convection vertical velocities may be of the order of more than $1\,\mathrm{m\,s^{-1}}$ – perhaps even 2–$5\,\mathrm{m\,s^{-1}}$ (Garratt 1992, p. 148; note that while $\hat{w}$ should be proportional to $\hat{U}$, it appears that it is numerically larger than the values quoted here for $\hat{U}$ or even $\hat{\hat{U}}$; we may therefore assume that $\hat{w}/\hat{U}$ is a fairly large number of order 20).

One criterion for the 'low-wind' regime would be

$$\hat{w} > w_\tau \sim 0.1U_{10};$$

with $\hat{w}$ of order $1\,\mathrm{m\,s^{-1}}$, this suggests that U_{10} must be less than about $10\,\mathrm{m\,s^{-1}}$, which roughly agrees with the observational evidence analysed in this paper.

More specifically we may write our criterion for prevalence of the 'weakly forced' convection regime as

$$\epsilon \sim \frac{w_\tau}{\hat{w}} \sim \mathrm{const.}\frac{U_{10}}{\hat{U}} \sim \frac{\mathrm{const.}}{C_H} \ll 1 \tag{9.6}$$

where C_H is the conventional heat exchange coefficient, and the constant (from the above discussion) is of order $0.05/20 \sim 0.002$. Interpreting (9.6) as a quantitative criterion is not without some arbitrariness, as the precise velocity and temperature differentials that go into C_H can be chosen in different ways. We may however note that, in the MONTBLEX data, C_H based on U_{10} and the temperature difference between 1 m and 10 m exceeds 0.04 at $U_{10} \lesssim 4\,\mathrm{m\,s^{-1}}$ (Rao *et al.* 1996*b*, figure 1), so the criterion above seems not unreasonable.

These arguments are not intended to be seen as 'proofs' in any sense, but do show that the overall approach adopted here is self-consistent.

10. Conclusion

We confirm here, by an analysis of atmospheric data, that at low wind speeds classical Monin–Obukhov theory, and in particular its limit as $u_* \to 0$, is unable to account for certain major characteristics of the eddy fluxes of momentum and heat. The observations show that, even at non-negligible wind speeds, the heat flux shows no strong correlation with wind speed, whereas the momentum flux varies linearly with wind speed. Monin–Obukhov theory cannot predict these marked features of the observed fluxes at low winds.

On the other hand, the approach adopted here postulates a regime of weakly forced or nearly free convection, in which the heat flux depends primarily on temperature differentials (and on wind only to a higher order), and the momentum flux results from a linear perturbation on pure free convection with no cross-wind. (A more detailed theoretical development of this argument will be published separately.) This suggests new heat-flux-based velocity scales for the flow; the classical friction velocity u_*, in the limit when it is small, is not the relevant scale in this point of view. Drag coefficients based on the new heat-flux velocity scales depend weakly or not at all on wind speed, showing a new kind of scaling in the weakly forced convection regime. The view implicit in the scaling proposed here is thus that the fluxes can generally be scaled on the basis of parameters close to the surface; the resulting velocities determine the overall boundary layer parameters. The temperature differences that determine the heat flux, however, will themselves be in general influenced by history and the large-scale environment.

We may finally ask what determines when the wind is sufficiently 'low' for the weakly forced convection regime to prevail. A plausible criterion is that a characteristic vertical velocity in free convection, say $\hat{w}$, must be high compared to the shear-driven vertical velocity fluctuation (say w_τ) scaled as in the fully forced convection regime.

In the present study it has been possible to analyse only the heat and momentum fluxes. It is easy to extend the study to cover moisture flux as well, as it closely follows laws similar to those for the heat flux. It is however necessary to extend the new similarity theory implicit in the present approach to other flow parameters and their variation with height; and this calls for new and careful measurements in the laboratory and in the atmosphere.

REFERENCES

BELJAARS, A. C. M. 1994 The parameterization of surface flux in large scale models under free convection. *Q. J. R. Met. Soc.* **121**, 255–270.

BRADLEY, E. F., COPPIN, P. A. & GODFREY, J. S. 1991 Measurements of sensible and latent heat flux in the western equatorial Pacific Ocean. *J. Geophys. Res. (Suppl.)* **96**, 3375–3389.

BUSINGER, J. A. 1973 Turbulent transfer in the atmospheric surface layer. In *Workshop on Micrometeorology* (ed. D. A. Haugen), pp. 67–100. American Meteorological Society.

BUSINGER, J. A., WYNGAARD, J. C., IZUMI, Y. & BRADLEY, E. F. 1971 Flux-profile relationship in the atmospheric surface layer. *J. Atmos. Sci.* **28**, 181–189.

DEARDORFF, J. W. 1972 Parameterization of the planetary boundary layer for use in general circulation models. *Mon. Weather Rev.* **2**, 93–106.

DEARDORFF, J. W. & WILLIS, G. W. 1985 Further results from a laboratory model of the convective planetary boundary layer. *Boundary-Layer Met.* **32**, 205–236.

EMANUEL, K. A. 1994 *Atmospheric Convection.* Oxford University Press.

FUKUI, K., KANAJIMA, M. & UEDA, H. A. 1983 A laboratory experiment on momentum and heat transfer in the stratified surface layer. *Q. J. R. Met. Soc.* **109**, 661–676.

GARRATT, J. R. 1978 Transfer characteristics for a heterogeneous surface of large aerodynamic roughness. *Q. J. R. Met. Soc.* **104**, 491–502.

GARRATT, J. R. 1992 *The Atmospheric Boundary Layer.* Cambridge University Press.

GEBHART, B. 1971 *Heat Transfer.* McGraw-Hill.

GERA, B. S., SINGAL, S. P., SAXENA, N. & RAMAKRISHNA, Y. S. 1996 Atmospheric boundary layer studies at Jodhpur during MONTBLEX using sodar and tower. *Proc. Ind. Acad. Sci. (Earth Planet. Sci.)* **105**, 261–272.

GODFREY, J. S. & BELJAARS, A. C. M. 1991 On the turbulent fluxes of buoyancy, heat and moisture at the air-sea interface at low wind speeds. *J. Geophys. Res.* **96**(C12), 22043-48.

GOEL, M. & SRIVASTAV, H. N. 1990 Monsoon Trough Boundary Layer Experiment (MONTBLEX). *Bull. Am. Met. Soc.* **71**, 1594–1600.

GRACHEV, A. A. 1989 Temperature profile and heat transfer in free turbulent convection along a horizontal surface. *Izv. Atm. Ocean Phys.* **25**, 132–140.

GRACHEV, A. A. 1990 Friction law in the free-convection limit. *Izv. Atm. Ocean Phys.* **26**, 837–846.

GRACHEV, A. A. & FAIRALL 2001 Upward momentum transfer in the marine boundary layer. *J. Phys. Oceanogr.* **31**, 1698–1711.

HACK, J. J., BOVILLE, B. A., BRIEGLEB, B. P., KIEHL, J. T., RASCH, P. J. & WILLIAMSON, D. L. 1993 Description of the NCAR Community Climate Model (CCM2). *NCAR Tech. Note* NCAR/TN-382+STR, NTIS PB93-221802/AS. Climate and Global Dynamics Division, National Center for Atmospheric Research, Boulder, Colorado.

HAUGEN, D. A. 1973 (Ed.) *Workshop on Micrometeorology.* American Meteorological Society.

INGERSOLL, A. P. 1966 Thermal convection with shear at high Rayleigh number. *J. Fluid Mech.* **25**, 209–228.

KAYS, W. M. & CRAWFORD, M. E. 1993 *Convective Heat and Mass Transfer.* McGraw-Hill.

KOMORI, S., UEDA, H., OGINO, F. & MIZUSHINA, T. 1982 Turbulent structure in unstably-stratified open-channel flow. *Phys. Fluids* **25**, 1539–1546.

KONDO, J. & ISHIDA, S. 1997 Sensible heat-flux from the Earth's surface under natural convective conditions. *J. Atmos. Sci.* **54**, 498–509.

KRAICHNAN, R. H. 1962 Turbulent thermal convection at arbitrary Prandtl number. *Phys. Fluids* **5**, 1374–1389.

MILLER, M. J., BELJAARS, A. C. M. & PALMER, T. N. 1992 The sensitivity of the ECMWF model to the parameterization of evaporation from the tropical oceans. *J. Climate* **5**, 418–434.

MONIN, A. S. 1970 The atmospheric boundary layer. *Annu. Rev. Fluid Mech.* **2**, 225–247.

MONIN, A. S. & YAGLOM, A. M. 1975 *Statistical Hydrodynamics.* MIT Press.

NARASIMHA, R., SIKKA, D. R. & PRABHU, A. 1997 *The Monsoon Trough Boundary Layer.* Indian Academy of Sciences, Bangalore.

Niemela, J. J., Skrbek, L., Sreenivasan, K. R. & Donnely, R. J. 2000 Turbulent convection at very high Rayleigh numbers. *Nature* **404**, 837–840.

Prandtl, L. 1932 Meteorologische Anwendung der Stromungslehre. *Beitr. Phys. Atmosph.* **19**, 188–202.

Rajkumar, G., Narasimha, R., Singal, S. P. & Gera, B. S. 1996 Thermal and wind structure of the monsoon trough boundary layer. *Proc. Ind. Acad. Sci (Earth Planet. Sci.)* **105**, 325–341.

Raju, H. V. & Narasimha, R. 2003 Limiting cross-flow velocity for heat flux to be determined by natural convection. *Intl J. Heat Mass Transfer* **46**, 4975–4978.

Rao, K. G. 1996 Roughness length and drag coefficient at two MONTBLEX-90 tower stations. *Proc. Ind. Acad. Sci. (Earth Planet. Sci.)* **105**, 273–287.

Rao, K. G. 2004 Estimation of the exchange coefficient of heat during low wind convective conditions. *Boundary-Layer Met.* **111**, 247–273.

Rao, K. G., Narasimha, R. & Prabhu, A. 1996*a* Estimation of drag coefficient at low wind speeds over the monsoon trough land region during MONTBLEX-90. *Geophys. Res. Lett.* **23**, 2617–2620.

Rao, K. G., Narasimha, R. & Prabhu, A. 1996*b* An analysis of MONTBLEX data on heat and momentum flux at Jodhpur. *Proc. Ind. Acad. Sci. (Earth Planet. Sci.)* **105**, 309–323.

Rudrakumar, S., Ameenulla, S. & Prabhu, A. 1995 MONTBLEX tower observations: Instrumentation, data acquisition and data quality. *Proc. Ind. Acad. Sci. (Earth Planet. Sci.)* **104**, 221–248.

Schumann, U. 1998 Minimum friction velocity and heat transfer in the rough surface layer of a convective boundary layer. *Boundary-Layer Met.* **44**, 311–326.

Sikka, D. R. & Narasimha, R. 1995 Genesis of the monsoon trough boundary layer experiment (MONTBLEX). *Proc. Ind. Acad. Sci. (Earth Planet. Sci.)* **104**, 157–187.

Srivastav, S. K. 1995 Synoptic meteorological observations and weather conditions during MONTBLEX-90. *Proc. Ind. Acad. Sci. (Earth Planet. Sci.)* **104**, 189–220.

Stull, R. B. 1988 *An Introduction to Boundary Layer Meteorology*. Kluwer.

Stull, R. B. 1994 A convective transport theory for surface fluxes. *J. Atmos. Sci.* **51**, 3–22.

Tennekes, H. 1973 Similarity laws and scale relations in planetary boundary layers. In *Workshop on Micrometeorology* (ed. D. A. Haugen), pp. 177–216. American Meteorological Society.

Townsend, A. A. 1959 Temperature fluctuations over a heated horizontal surface. *J. Fluid Mech.* **5**, 209–41.

Townsend, A. A. 1964 Natural convection on water over an ice surface. *Q. J. R. Met. Soc.* **90**, 248–259.

Townsend, A. A. 1972 Mixed convection over a heated horizontal plane. *J. Fluid Mech.* **55**, 209–227.

Turner, J. S. 1973 *Buoyancy Effects in Fluids*. Cambridge University Press.